# Sensor Fault Accommodation for a Plug Flow Reactor using an M-Estimator

**Gaurav Seth**[a], **Pavanraj H. Rangegowda**[b], **Sachin C. Patwardhan**[a] *, **Mani Bhushan**[a]

[a] *Department of Chemical Engineering, IIT Bombay, Powai, Mumbai-400076, India.*
[b] *Bhabha Atomic Research Centre, Homi Bhabha National Institute, Mumbai-400094,India.*

**Abstract:** The presence of gross errors in the measurements can lead to biased state estimates when conventional Bayesian estimators are used. This can hamper the model-based monitoring and control schemes that rely on the accurate state estimates. In this work, we have developed a framework for robust estimation of the state profiles for Distributed parameter systems (DPSs), in the presence of biased measurements. The proposed approach uses an M-estimator to identify the faulty sensor. The sensor fault diagnosis is then used to augment the state estimator with an extra state that estimates the drifting sensor bias. The proposed approach has been applied to an Auto-Thermal tubular reactor system. The proposed scheme successfully isolates the biased temperature sensors and includes or removes additional bias states as and when required. The gross errors/biases are estimated and subsequently accommodated to provide accurate estimates of spatial profiles of reactor concentration and temperature.

*Keywords:* Fault detection, distributed parameter system, M-estimator

## 1. INTRODUCTION

Online estimation of state profiles of the system is an essential part of any model based monitoring and control schemes for distributed parameter systems (DPSs). The quality of the measurements obtained from the plant is critical to the efficacy of the estimator. In practice, the measurements available can be corrupted with gross errors such as outliers, biases, and drifts that may arise due to miscalibration, fouling of sensors, or fluctuations in some parameters. These gross errors can lead to biased estimates of the state profiles. However, relatively limited literature can be found on the sensor fault diagnosis and accommodation for DPSs (Ferdowsi et al. (2019)).

When the measurements are susceptible to gross errors, a sensor fault diagnosis framework is required to negate the impact of these unknown uncertainties on state estimates. Many fault diagnosis schemes are available in the literature for the lumped parameter systems (LPSs) based on Bayesian state estimation schemes. These include active approaches that involve isolating the source of gross error, estimating its magnitude, and explicitly compensating for the gross errors in the measurements while performing state estimation for the system (Rangegowda et al. (2020)). Passive approaches, on the other hand, make the state estimates insensitive to the gross errors in the measurements by eliminating the biased sensor (Valluru et al. (2018)). These approaches integrate a Maximum-likelihood type estimator (or M-estimator) along with the Bayesian state estimators to make estimates robust to gross errors in the measurements. The robust estimation schemes, in general, eliminate the use of faulty measurements which leads to loss of information.

In this work, we have proposed an active method for sensor fault diagnosis of a DPSs by combining an M-estimator with a conventional state estimation scheme. The ability of the M-estimator to block a faulty sensor is used to isolate the faulty sensor. Subsequently, the bias present in the sensor measurements is estimated using the random walk model in combination with the state estimator. Thus, the proposed scheme makes use of the biased measurement for state estimation with implicit (or active) bias compensation. A reduced-order model of a DPSs is constructed using the orthogonal collocation (OC) technique and further used to develop a DAE-EKF that uses measurements distributed throughout the spatial domain for the reconstruction of state profiles (Seth et al. (2021)). An M-estimator is used in parallel for the identification of faulty sensor(s). M-estimators are robust to the gross errors in the measurements as the influence function of these estimators is bounded even when the bias magnitudes become large (de Menezes et al. (2021)). The proposed approach uses the information of the gradient of the influence function of the chosen M-estimator for sensor fault detection. Once the occurrence of a sustained gross error in a sensor is confirmed, the state-space model is augmented with an additional state for simultaneous estimation of the bias. Further, disappearance of the bias in the measurement is detected using hypothesis testing and the augmented state is removed when the bias magnitude is reduced to zero. The proposed active approach continues to use the biased measurement for state profile reconstruction. The proposed approach can

* Corresponding author (e-mail: sachinp@iitb.ac.in)

deal with multiple faulty sensors, where the biases can occur sequentially in time.

Rest of the paper is organized as follows: Section 2 gives the details of the process model used for simulations. Section 3 gives the methodology applied for sensor fault diagnosis. Simulation results are presented in Section 4 and main conclusions of the work are given in Section 5.

## 2. PROCESS MODEL

In general the dynamics of a DPSs is represented by a set of PDEs along with the boundary conditions and initial conditions. The dynamic system considered in this work can be represented by the set of coupled PDEs given by Eq. (1) along with the boundary and initial conditions (Eq. (2)-Eq. (5)) given as:

$$\frac{\partial x_r(z,t)}{\partial t} = f_r\left(\frac{\partial x_r(z,t)}{\partial z}, \frac{\partial^2 x_r(z,t)}{\partial z^2}, \mathbf{x}(z,t), \mathbf{u}(t)\right) \quad (1)$$

$$g_r\left[\frac{dx_r}{dz}, \mathbf{x}(0,t), \mathbf{u}(t)\right] = 0 \qquad \text{at } z = 0 \quad (2)$$

$$h_r\left[\frac{dx_r}{dz}, \mathbf{x}(1,t), \mathbf{u}(t)\right] = 0 \qquad \text{at } z = 1 \quad (3)$$

$$\text{where, } 1 \leq r \leq n \quad (4)$$

$$x_1(z,0) = a_1(z), x_2(z,0) = a_2(z), ..., x_n(z,0) = a_n(z) \quad (5)$$

Here, $\mathbf{x} = [x_1, ..., x_r, ..., x_n]^T$ is the state vector containing $n$ state variables and $x_r$ denotes the $r^{th}$ state variable of the system, $t \in [0, \infty)$ denotes the temporal domain, and $z \in [0, 1]$ denotes the spatial domain, $\mathbf{u}(t)$ denotes the vector of manipulated inputs to the system. To analyze such systems a common approach is to discretize the PDEs to a reduced order model consisting of differential and algebraic equations (DAEs).

### 2.1 Reduced Dimensional Model

Using $(N+1)^{th}$ order Lagrange polynomial and its derivatives for discretizing the PDEs in spatial domain, a reduced order model can be constructed as follows (Seth et al. (2021)):

$$\frac{d\chi_{r,i}(t)}{dt} = f_r(\mathbf{L}'(\xi_i)\boldsymbol{\chi}_r, \mathbf{L}''(\xi_i)\boldsymbol{\chi}_r, \boldsymbol{\chi}(\xi_i,t), \mathbf{u}(t), \mathbf{d}(t)) \quad (6)$$

$$2 \leq i \leq N \text{ and } 1 \leq r \leq n$$

$$g_r\left[\mathbf{L}'(\xi_1)\boldsymbol{\chi}_r, \boldsymbol{\chi}(\xi_1,t), \mathbf{u}(t)\right] = 0 \qquad at\ \xi = \xi_1 \quad (7)$$

$$h_r\left[\mathbf{L}'(\xi_{\mathcal{N}+1})\boldsymbol{\chi}_r, \boldsymbol{\chi}(\xi_{\mathcal{N}+1},t), \mathbf{u}(t)\right] = 0 \qquad at\ \xi = \xi_{N+1} \quad (8)$$

$$\text{for } 1 \leq r \leq n$$

where, $\boldsymbol{\chi}_r = [\chi_{r,1}, \chi_{r,2}, ..., \chi_{r,N+1}]^T$ is the vector containing the values for $r^{th}$ state variable at the collocation points ($\xi_i$) where, $\chi_r(\xi_i) = \chi_{r,i}$ is the value of $r^{th}$ state variable at $i^{th}$ collocation point. $\boldsymbol{\chi} = [\chi_{1,1}, ..., \chi_{1,N+1}, ..., \chi_{n,1}, ..., \chi_{n,N+1}]^T$ or $[\boldsymbol{\chi}_1^T, ..., \boldsymbol{\chi}_r^T, ..., \boldsymbol{\chi}_n^T]^T$ represents the augmented state vector. $\mathbf{L}'(\xi_i)$ and $\mathbf{L}''(\xi_i)$ represents the vectors of coefficients for first and second derivatives of the Lagrange polynomial, calculated at $i^{th}$ collocation point respectively. Further, this reduced-order model can be represented in a discrete time form as follows:

$$\boldsymbol{\chi}_{d,k} = \mathbf{F}(\boldsymbol{\chi}_{d,k-1}, \boldsymbol{\chi}_{a,k-1}, \mathbf{u}_{k-1}) + \mathbf{w}_{k-1} \quad (9)$$

$$\mathbf{0}_{2n\times 1} = \boldsymbol{\Lambda}(\boldsymbol{\chi}_{d,k}, \boldsymbol{\chi}_{a,k}, \mathbf{u}_{k-1}) \quad (10)$$

where,

$$\mathbf{F}(\boldsymbol{\chi}_{d,k-1}, \boldsymbol{\chi}_{a,k-1}, \mathbf{u}_{k-1}) = \boldsymbol{\chi}_{d,k-1} + \int_{(k-1)T_s}^{kT_s} \mathbf{f}(\boldsymbol{\chi}_d, \boldsymbol{\chi}_a, \mathbf{u}_{k-1})dt \quad (11)$$

Here, $k = 0, 1, 2, ...$ represents the discrete sampling instants, $\mathbf{F}$ and $\boldsymbol{\Lambda}$ are the differential and algebraic operators of the discrete time system, $\mathbf{w}_{k-1} \sim \mathcal{N}(\mathbf{0}, \mathbf{Q_w})$ is Gaussian noise affecting the differential states of the system with noise covariance matrix $\mathbf{Q_w}$, $T_s$ is the sampling interval of the system, $\boldsymbol{\chi}_d \in \mathbb{R}^{n_d}$, $n_d = n(N-1)$, represents the values of the differential states, obtained at the internal collocation points ($2 \leq i \leq N$) and $\boldsymbol{\chi}_a \in \mathbb{R}^{n_a}$, $n_a = 2n$, represents the values of algebraic states obtained from the boundary conditions of the system ($i = 1$ and $i = N+1$). The vectors $\boldsymbol{\chi}_d$ and $\boldsymbol{\chi}_a$ can be further combined to form the augmented state vector $\boldsymbol{\chi} \in \mathbb{R}^{n(N+1)}$. Note that $\boldsymbol{\chi}$ gives the state values at only collocation points. $\mathbf{u} \in \mathbb{R}^{n_u}$ represents the manipulated inputs.

### 2.2 Measurement Model

It is to be noted that the spatial locations of the sensors need not correspond to the location of the collocation points. Thus, to develop the measurement model, it requires the development of relationships between the states and the measurements. Thus, the measurement matrix, $\mathbf{C}$, that relates the states with the outputs is obtained by interpolation using the Lagrange polynomials constructed using differential and algebraic states. Details of construction of matrix $\mathbf{C}$ can be found in Seth et al. (2021). Further, the measurements are assumed to be obtained at regular sampling intervals and are given by Eq. (12):

$$\mathbf{Y}_k = \mathbf{C}\boldsymbol{\chi}_k + \mathbf{v}_k \quad (12)$$

where, $\mathbf{C} = [blkdiag(\mathcal{C}_1, ..., \mathcal{C}_r, ..., \mathcal{C}_n)]$ and $\mathcal{C}_r$ is the measurement matrix for the $r^{th}$ state variable and $\mathbf{v}_k \in \mathbb{R}^m$ represents the measurement noise at instant $k$, which is modeled as zero mean Gaussian white noise with covariance matrix $\mathbf{R}$.

As mentioned earlier the measurements can occasionally be corrupted with bias. Assuming that a drifting bias in the $s^{th}$ sensor occurs at instant $k_{s0}$, the measured outputs after the occurrence of the bias can be represented as:

$$\mathbf{Y}_k = \mathbf{C}\boldsymbol{\chi}_k + \mathbf{v}_k + \beta_{s,k}\mathbf{e}_{s,k}\sigma_s(k - k_{s0}),\ k \geq k_{s0} \quad (13)$$

where, $\beta_{s,k}$ represents the time varying magnitude of the bias occurring in the $s^{th}$ sensor. Note that bias magnitude can vary with the sampling instants $k \geq k_{s0}$ and $\mathbf{e}_{s,k} \in \mathbb{R}^m$ is a unit vector which is defined as:

$$\mathbf{e}_{s,k} = [0, ..., 1, ..., 0]^T \quad (14)$$

where the $s^{th}$ element is 1 and rest are zero. Here, $\sigma_s(k - k_{s0})$ represents a unit step function, defined as:

$$\sigma_s(k - k_{s0}) = \begin{cases} 0 \text{ if } k < k_{s0} \\ 1 \text{ if } k \geq k_{s0} \end{cases} \quad (15)$$

Similarly, if at a later instant $k_{j0}$, a bias occurs in the $j^{th}$ sensor, then the corresponding measurement variation will be represented as: $\mathbf{Y}_k = \mathbf{C}\boldsymbol{\chi}_k + \mathbf{v}_k + \beta_{j,k}\mathbf{e}_{j,k}\sigma_j(k - k_{j0})$.

In this work, the reduced DAEs model (Eqs. (9) - (11)) together with measurement models Eqs. ((12) - (15)) are used for simulating plant behavior. Also, the reduced DAEs model (Eqs. (9) - (11)) and the measurement model Eq. (12) are used to develop EKF under the fault free conditions.

## 3. SENSOR FAULT TOLERANT STATE ESTIMATION

In the absence of biased measurements, state estimation is carried out using Extended Kalman Filter for DAEs system (DAE-EKF) (Mandela et al. (2010)).

Prediction Step:

$$\widehat{\boldsymbol{\chi}}_{d,k|k-1} = \mathbf{F}(\widehat{\boldsymbol{\chi}}_{d,k-1|k-1}, \widehat{\boldsymbol{\chi}}_{a,k-1|k-1}, \mathbf{u}_{k-1}) \tag{16}$$

$$\mathbf{0}_{2n\times 1} = \boldsymbol{\Lambda}(\widehat{\boldsymbol{\chi}}_{d,k|k-1}, \widehat{\boldsymbol{\chi}}_{a,k|k-1}, \mathbf{u}_{k-1}) \tag{17}$$

$$\mathbf{P}_{k|k-1} = \boldsymbol{\Phi}_{k-1}\mathbf{P}_{k-1|k-1}\boldsymbol{\Phi}_{k-1}^T + \boldsymbol{\Gamma}_{k-1}\mathbf{Q}_{\mathbf{w}}\boldsymbol{\Gamma}_{k-1}^T \tag{18}$$

Update Steps:

$$\widehat{\boldsymbol{\chi}}_{k|k} = \widehat{\boldsymbol{\chi}}_{k|k-1} + \mathbf{K}_k(\mathbf{Y}_k - \mathbf{C}\widehat{\boldsymbol{\chi}}_{k|k-1}) \tag{19}$$

$$\mathbf{P}_{k|k} = (\mathbf{I} - \mathbf{K}_k\mathbf{C})\mathbf{P}_{k|k-1} \tag{20}$$

where, $\mathbf{K}_k$ is the kalman gain defined as:

$$\mathbf{K}_k = \mathbf{P}_{k|k-1}\mathbf{C}^T(\mathbf{C}\mathbf{P}_{k|k-1}\mathbf{C}^T + \mathbf{R})^{-1} \tag{21}$$

For consistency of algebraic states, only the updated differential state vector $\widehat{\boldsymbol{\chi}}_{d,k|k}$ obtained using Eq. (19) is retained and the algebraic states are computed from the Eq. (10). Finally, the updated state vector is transformed to construct $n$ continuous functions $(\widehat{\chi}_1(z), \widehat{\chi}_2(z), ..., \widehat{\chi}_n(z))$, each of which represents the estimated spatial state profile of the system as a function of spatial variable $z$.

$$\widehat{\mathbb{X}}_k(z) = \mathcal{L}_z\widehat{\boldsymbol{\chi}}_{k|k} \tag{22}$$

where,

$$\mathcal{L}_z = [blkdiag(\mathbf{L}_z^T, \mathbf{L}_z^T, ..., \mathbf{L}_z^T)]_{n\times n(N+1)} \tag{23}$$

$$\mathbf{L}_z = \begin{bmatrix} L_1(z) & L_2(z) & \dots & L_{N+1}(z) \end{bmatrix}^T \tag{24}$$

where, $L_1(z), L_2(z), ..., L_{N+1}(z)$ are the Lagrange polynomial coefficients of $(N+1)^{th}$ order Lagrange polynomial and $\widehat{\mathbb{X}}_k(z) = \begin{bmatrix} \widehat{\chi}_1(z) & \widehat{\chi}_2(z) & \dots & \widehat{\chi}_n(z) \end{bmatrix}^T$. Thus, an estimate of the state profile over the entire spatial domain can be constructed (Seth et al. (2021)).

### 3.1 Biased Sensor Isolation using M-estimator:

An M-estimator is defined as the function of a normalized measurement error or studentized error vector, i.e., the difference between the actual and estimated measurement normalized by the standard deviation. At $k^{th}$ instant it can be defined as:

$$\boldsymbol{\zeta}_k = \mathbf{S}^{-1}[(\mathbf{Y}_k - \mathbf{C}\boldsymbol{\chi}_k)] \tag{25}$$

where

$$\mathbf{S} = \mathbf{R}^{\frac{1}{2}} = diag[\sigma_1, ..., \sigma_s, ..., \sigma_m] \tag{26}$$

Here, $\sigma_s$ represents the standard deviation of the measurement noise in the $s^{th}$ sensor and $diag[.]$ operator represents a diagonal matrix constructed using the diagonal elements of the matrix argument.

In the present work the Hampel's three part redescending estimator is considered. For $s^{th}$ sensor measurement of $\boldsymbol{\zeta}_k$ i.e., $\zeta_{k,s}$, where $s = 1, 2, ..., m$, the redescending estimator can be defined as follows:

$$\rho_{k,s}(\zeta_{k,s}) = \begin{cases} \frac{1}{2}\zeta_{k,s}^2, & 0 \le |\zeta_{k,s}| \le a \\ a|\zeta_{k,s}| - a^2/2, & a < |\zeta_{k,s}| \le b \\ ab - \frac{a^2}{2} + \frac{a(c-b)}{2}\left[1 - \left(\frac{c - |\zeta_{k,s}|}{(c-b)}\right)^2\right], & b < |\zeta_{k,s}| \le c \\ ab - \frac{a^2}{2} + \frac{a(c-b)}{2}, & |\zeta_{k,s}| > c \end{cases} \tag{27}$$

where $(a, b, c)$ are the three tuning parameters which satisfy the condition $c \ge b + 2a$. Details of the tuning of these parameters can be referred from Valluru et al. (2018). The influence function , $\Psi(\zeta_{k,s})$, (which is proportional to the first derivative of the M-estimator) is the measure of the robustness of any given M-estimator. Behavior of

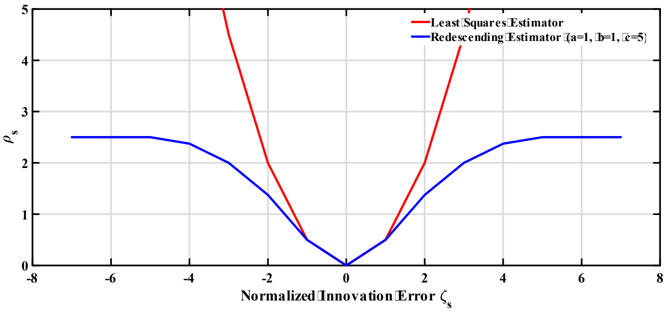


Fig. 1. Comparison of Hampel's redescending estimator with Least squares estimator

redescending estimator with normalized error is demonstrated by Figure (1) where it is compared with the least squares estimator. It can be observed that as the absolute value of normalized error $|\boldsymbol{\zeta}_{k,s}|$ becomes larger, the redescending estimator becomes bounded, thereby indicating the robustness of redescending estimator to large measurement errors. Also, as the normalized errors corresponding to the $s^{th}$ sensor crosses a threshold value, the gradient of influence function $\nabla\Psi(\zeta_{k,s})$ becomes negligible (ref: Appendix). Therefore, by using the information of gradient of the influence function $\nabla\boldsymbol{\Psi}(\boldsymbol{\zeta}_k)$, i.e.,

$$\nabla\boldsymbol{\Psi}(\boldsymbol{\zeta}_k) = \left[\frac{\partial\Psi(\zeta_{k,1})}{\partial\zeta_{k,1}}, ..., \frac{\partial\Psi(\zeta_{k,m})}{\partial\zeta_{k,m}}\right]^T \tag{28}$$

the sensor which is biased is detected.

Since the true states $\boldsymbol{\chi}_k$ defined in normalized measurement error vector Eq. (25) are unknown, in this work, we propose to use the normalized innovation sequence for constructing the M-estimator. Hence, the normalized innovation error vector is defined as:

$$\boldsymbol{\zeta}_k \approx (\boldsymbol{\Sigma}_k)^{-1}[(\mathbf{Y}_k - \mathbf{C}\widehat{\boldsymbol{\chi}}_{k|k-1})] \tag{29}$$

$$where, \boldsymbol{\Sigma}_k = (\ diag[\mathbf{P}_{E,k}])^{\frac{1}{2}} \tag{30}$$

$$\mathbf{P}_{E,k} = (\mathbf{C}\mathbf{P}_{k|k-1}\ \mathbf{C}^T + \mathbf{R}) \tag{31}$$

Here, $\boldsymbol{\Sigma}_k$ is defined by taking an approximation of $\mathbf{P}_{E,k}$ under the assumption that the off diagonal elements are relatively small and only the diagonal elements of matrix $\mathbf{P}_{E,k}$ are considered.

After the detection of biased sensor (lets say $s^{th}$ sensor is detected to be faulty), we observe the corresponding value of the gradient of the influence function i.e., $\nabla\Psi(\zeta_{k,s})$ over the window of $n_f$ sampling instants. This is referred to as fault confirmation window. If the majority of the values of $\nabla\Psi(\zeta_{k,s})$ in the fault confirmation window appear to be zero (indicating that the measurements from the sensor are faulty) then the sensor is confirmed to be biased at instant $k_{s,c} \geq k_{s0} + n_f$. This is done to differentiate whether the variation in measurements are due to some random error or due to the presence of gross errors. Once the bias in the sensor is confirmed, further correction is performed to reduce the effect of bias measurements on the state profile estimates. Although, in this work, we have used the Hampel's redescending M-estimator, the approach presented can also be implemented using other M-estimators.

*3.2 Estimating and Accommodating the Bias Estimates:*

Assuming that bias in the $s^{th}$ sensor has been confirmed at sampling instant $k \geq k_{s,c}$, we augment the state dynamics vector, $\boldsymbol{\chi}_k$ with an extra variable for the sensor bias and the resulting augmented vector is given as: $\mathbf{X}_k = \left[\, \boldsymbol{\chi}_k^T \;\; \beta_{s,k}^T \,\right]^T$.This is achieved under the assumption that the sensor bias is modelled as a random walk process, i.e.,

$$\beta_{s,k} = \beta_{s,k-1} + w_{\beta,k-1} \tag{32}$$

where, $\beta_{s,k}$ is the magnitude of bias in the $s^{th}$ sensor occurring at $k^{th}$ sampling instant, and $w_{\beta,k-1}$ is assumed to be zero mean Gaussian distribution with variance as $Q_\beta$, which is treated as a tuning parameter. The DAE-EKF algorithm is then applied for the augmented system with the state noise covariance matrix modified as follows:

$$\mathbf{Q}_{k-1} = blkdiag(\boldsymbol{\Gamma}_{k-1}\mathbf{Q}_{\mathbf{w}}\boldsymbol{\Gamma}_{k-1}^T, Q_\beta) \tag{33}$$

and the augmented measurement matrix $C_k$ modified as follows:

$$C_k = [\, \mathbf{C} \;\; \mathbf{e}_{s,k} \,] \tag{34}$$

where, $\mathbf{e}_{s,k}$ is defined in the section 2.2. The resulting updated augmented state vector $\widehat{\mathbf{X}}_{k|k}^T$ is a stacked vector of estimates of updated state vector $\widehat{\boldsymbol{\chi}}_{k|k}$ and the updated bias magnitude corresponding to the $s^{th}$ sensor, $\widehat{\beta}_{s,k}$, i.e.,

$$\widehat{\mathbf{X}}_{k|k} = \left[\, \widehat{\boldsymbol{\chi}}_{k|k}^T \;\; \widehat{\beta}_{s,k}^T \,\right]^T \tag{35}$$

Similarly, if the bias occurs in the $j^{th}$ sensor, it can be estimated and corrected for by modifying $C_k$, by replacing $\mathbf{e}_{s,k}$ with $\mathbf{e}_{j,k}$ and so on. For consistency of algebraic states, the differential state vector $\widehat{\boldsymbol{\chi}}_{d,k|k}$ is retained and the algebraic states are computed from the Eq.(10). Further it is transformed to the spacial state profiles using Eq. (22).

*3.3 Hypothesis Testing*

In case when the sensor bias is restored to zero value, we no longer need the augmented structure and evaluate the bias estimates. So, we can remove the additional state when we have bias free measurements. To verify the absence of bias in the measurements at $k^{th}$ sampling instant, we perform two-tailed t-test on the sample of bias estimates of size $p$, i.e., $\widehat{\beta}_{s,k-p+1}, \widehat{\beta}_{s,k-p+2}, ..., \widehat{\beta}_{s,k}$. Assuming that the sample of estimates considered is derived from a Gaussian distribution with mean $\mu$ and unknown variance, the t-test is performed to test the following hypotheses:

$$H_0 : \mu = 0 \quad \text{and} \quad H_1 : \mu \neq 0 \tag{36}$$

The t-score ($\tau_{[k-p+1,k]}$) for the test over the time window $[k-p+1, k]$ is given as:

$$\tau_{[k-p+1,k]} = \frac{\sqrt{p}}{\widehat{\sigma}_{\beta,k}} \left|\overline{\beta}\right| \quad \text{where} \quad \overline{\beta} = \frac{\sum_{i=1}^{p} \widehat{\beta}_{s,k-p+i}}{p} \tag{37}$$

where, $\widehat{\sigma}_{\beta,k}^2$ is the sample variance over the time window $[k-p+1, k]$. We accept the null hypothesis i.e, we can claim that bias in the sensor has reduced to zero if $\tau_{[k-p+1,k]} \leq t_{\alpha/2,p-1}$, where $t_{\alpha/2,p-1}$ is the critical value that is determined by the significance level $\alpha$ and the degrees of freedom $(p-1)$.

## 4. SIMULATION STUDIES

In this section, we demonstrate the performance of the proposed algorithm for identifying the biased sensor as well as quantifying the amount of gross error. Simulation studies are carried out on an Auto-Thermal tubular reactor system which is a two state system namely, dimensionless concentration ($C$) and dimensionless temperature ($T$). The coupled PDEs governing the pseudo homogeneous dynamic model of the system is given in Berezowski et al. (2000). For our simulation purpose following values of various parameters have been used (Pacharu et al. (2012)): $Pe_m = 100$; $Pe_T = 100$; $T_{H_0} = 0$; $\delta = 2$; $\psi = 0.3$; $Da = 0.15$; $\kappa = 2$; $\gamma = 10$; $\omega = 1.4$. The PDEs are spatially discretized at 11 internal collocation points space i.e , $N + 1 = 13$. This results in 22 differential states and 4 algebraic states. The temperature of cooling medium ($T_H$) is treated as manipulated input and assumed to vary as PRBS signal with frequency range $[\, 0 \;\; 0.1 \,]$ and the nominal value $T_{H_0} = 0$ units. Only temperature measurements were assumed to be available from the 6 sensors placed at equidistant spatial locations given as: $0, 0.2, 0.4, 0.6, 0.8$ and 1. Other relevant filter parameters are: $\mathbf{Q}_{\mathbf{w}} = 0.001^2 \times \mathbf{I}_{2(N-1)\times 2(N-1)}, \mathbf{R} = 0.005^2 \times \mathbf{I}_{6\times 6}, Q_\beta = 0.004^2$. The simulations were carried out for 500 sampling instants ($T_s = 0.1$). The measurements from $2^{nd}$ and $4^{th}$ sensors were assumed to be corrupted with biases varying differently with time. The length of the fault confirmation window is chosen as $n_f = 5$.. Hypothesis testing is performed with 95% confidence interval and 20 degrees of freedom i.e., p = 21. The tuning parameters for the M-estimator used for simulation purposes are, $a = 1$, $b = 1$ and $c = 5$. The biases introduced in the $2^{nd}$ and $4^{th}$ sensors and the corresponding estimates obtained from the proposed algorithm are given by Figure (2) and Figure (3) respectively.

To check the effectiveness of the proposed approach, state estimates for the two different filter implementations have been considered:

**Case A:** State profile estimation under the influence of biased measurements using DAE-EKF without fault diagnosis and bias estimation.

**Case B:** State profile estimation under the influence of biased measurements using DAE-EKF and M-estimator for fault diagnosis and accommodation.

In case B, the biases in the sensors have been accurately estimated as shown in Figures 2 and 3. Note that the bias estimation starts only after the bias in the sensors is confirmed and further simultaneous DAE-EKF is used for estimating both states and the bias in sensors. Further from these figures it is noted that the biases in the sensors are estimated till the gross error in the sensor(s) reduces to zero and stops after confirmation of the availability of the unbiased measurements by performing the hypothesis test given in section 3.4. Figures 4 and 5 represent the comparison of true states, biased measurements and the state estimates of the reactor temperature ($T$), obtained for both the cases. The comparison has been made at the locations where biased sensors are assumed to be placed. As can be inferred from the Figures, the proposed algorithm works efficiently in estimating the true values of the states even when the measurements obtained from the sensors are corrupted with gross errors. The confirmation of the biased measurements and subsequent correction to obtain the accurate estimates of the states can also be noticed from Figures 4 and 5. Figure (6) shows the variation of innovation errors for the faulty sensors evaluated for both the cases. It can be seen that for case B, innovations for both the faulty sensors are reduced to zero mean immediately after the occurrence of bias, even though the measurements obtained from the plant continues to be biased. Further it can be seen that the bias present in one of the sensors can also effect the innovations computed using other sensors since the biased measurements from any sensor will effect the state estimates throughout the spatial domain.

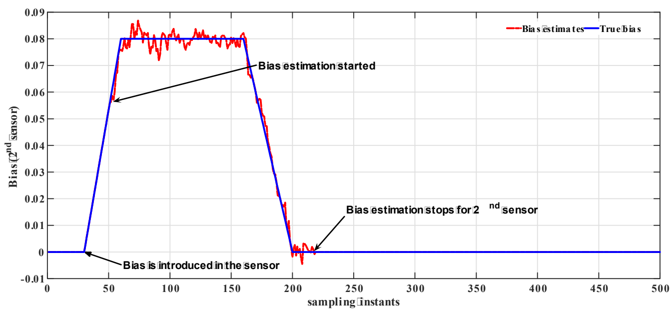


Fig. 2. Bias introduced in the $2^{nd}$ sensor and the corresponding estimates

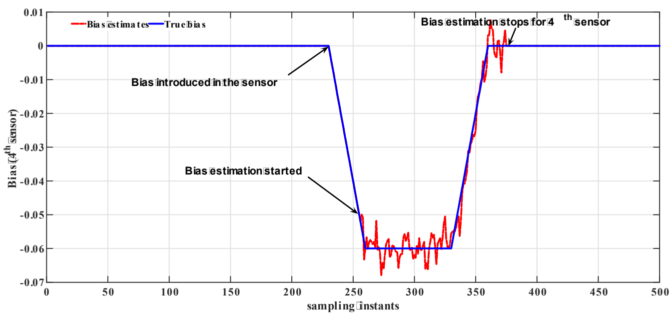


Fig. 3. Bias introduced in the $4^{th}$ sensor and the corresponding estimates

The state profile estimates at $100^{th}$ sampling instant (when $2^{nd}$ sensor is biased) is also compared for both the

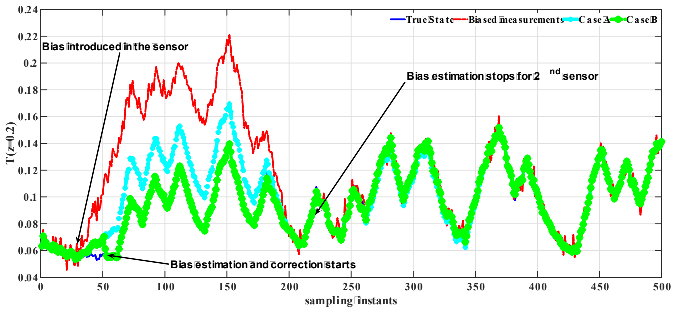


Fig. 4. Comparison of true states, biased measurements and state estimates obtained for both the cases for $2^{nd}$ sensor ($z = 0.2$)

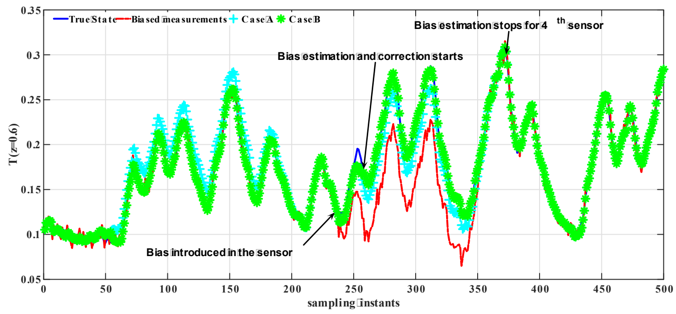


Fig. 5. Comparison of true states, biased measurements and state estimates obtained for both the cases for $4^{th}$ sensor ($z = 0.6$).

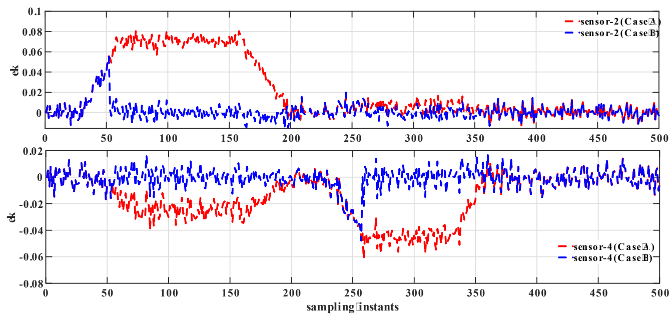


Fig. 6. Variation of innovation error for the faulty sensors for both the cases a) $2^{nd}$ sensor b) $4^{th}$ sensor

case studies in Figure (7). The profile estimates obtained corresponding to Case B are fairly accurate for both the measured as well as unmeasured state variables while the estimates obtained from Case A are highly inaccurate.

The estimation performance of the proposed algorithm was also examined by evaluating the root profile estimation squared error (RPSE) defined as follows:

$$\mathrm{RPSE}(k) = \sqrt{\int_0^1 (\mathrm{PSE}(z))dz} \tag{38}$$

where,

$$PSE(z) = \left\{ \mathbf{L}_z \left( \boldsymbol{\chi}_{r,k} - \widehat{\boldsymbol{\chi}}_{r,k|k} \right) \right\}^2$$

where, $\mathbf{L}_z \left( \boldsymbol{\chi}_{r,k} - \widehat{\boldsymbol{\chi}}_{r,k|k} \right)$ defines the profile error as a function of spatial variable $z$ for the $r^{th}$ state variable at $k^{th}$ sampling instant. At $k^{th}$ sampling instant, Eq.(38)

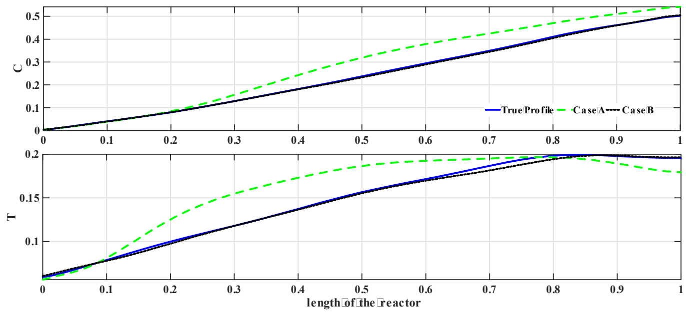


Fig. 7. Profile estimates for dimensionless concentration (C) and dimensionless temperature (T) obtained at $100^{th}$ sampling instant for both the case studies.

gives the root of integrated value of the squared estimation error calculated throughout the spatial domain. The RPSE values for dimensionless concentration $(C)$ and dimensionless temperature $(T)$ obtained for both the case studies are represented in Figure (8). It is evident from the Figure that for case B, the effects of biased measurements on the profile estimates of both the measured and the unmeasured states are reduced soon after the appearance of bias in the sensors.

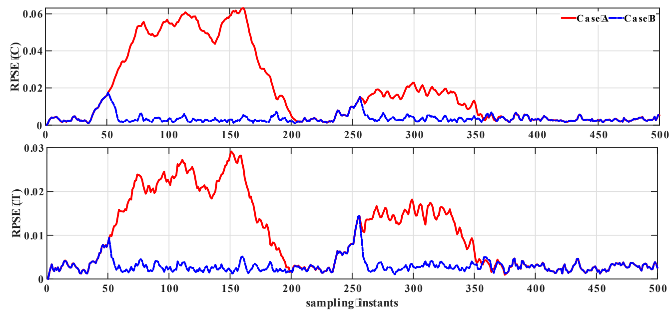


Fig. 8. RPSE values for dimensionless concentration (C) and dimensionless temperature (T) for both the cases.

## 5. CONCLUSIONS

In this work, a framework for estimating the state profiles of a Distributed Parameter system is developed which is robust to the gross errors or bias in the measurements. A tubular reactor case study involving the occurrence of biases in two sensors placed at different locations in space is considered to investigate the performance of the proposed algorithm. From the results it can be claimed that a properly tuned M-estimator can be employed parallelly to the EKF to quickly identify and isolate the faulty sensor in a spatially distributed system. The proposed algorithm automates the fault detection, isolation and magnitude estimation by explicitly incorporating it with simultaneous DAE-EKF algorithm and correct the biased measurements. The augmentation is carried out by adding or removing an additional state variable as and when a bias in a sensor is detected and the bias reduces to zero. Simulation results presented in the work shows that fairly accurate state profile estimates of the system are obtained by using the proposed framework in the presence of a biased sensor. Results presented in this work reveal that the framework developed can work efficiently with sequential bias occurring in one or more sensors. Moreover, unlike the conventional M-estimator based schemes that eliminate the faulty sensor measurement, the proposed approach continues to use the biased measurement for state estimation thereby preventing any loss of information. Thus, the proposed algorithm is suited for accurate estimates of the state profiles of a distributed parameter system unaffected by the biased measurements.

## Appendix- 1

The influence function, $\Psi(\zeta_{k,s})$ and its gradient $\nabla\Psi(\zeta_{k,s})$ for the redescending estimator are given as follows:

$$\Psi(\zeta_{k,s}) = \begin{cases} \zeta_{k,s}, & 0 \le |\zeta_{k,s}| \le a \\ \pm a, & a < |\zeta_{k,s}| \le b \\ \dfrac{\pm a\,(c - |\zeta_{k,s}|)}{c-b}, & b < |\zeta_{k,s}| \le c \\ 0, & |\zeta_{k,s}| > c \end{cases} \tag{39}$$

$$\nabla\Psi(\zeta_{k,s}) = \frac{\partial\Psi(\zeta_{k,s})}{\partial\zeta_{k,s}} = \begin{cases} 1, & 0 \le |\zeta_{k,s}| \le a \\ 0, & a < |\zeta_{k,s}| \le b \\ \dfrac{-a}{c-b}, & b < |\zeta_{k,s}| \le c \\ 0, & |\zeta_{k,s}| > c \end{cases} \tag{40}$$

## REFERENCES

Berezowski, M., Ptaszek, P., Jacobsen, E. W., 2000. Dynamics of heat-integrated pseudohomogeneous tubular reactors with axial dispersion. Chemical Engineering and Processing: Process Intensification 39 (2), 181–188.

de Menezes, D. Q. F., Prata, D. M., Secchi, A. R., Pinto, J. C., 2021. A review on robust M-estimators for regression analysis. Computers & Chemical Engineering 147, 1–30.

Ferdowsi, H., Cai, J., Jagannathan, S., 2019. Fault Detection and Estimation for a Class of Nonlinear Distributed Parameter Systems. IEEE International Conference on Prognostics and Health Management (ICPHM), 1–8.

Mandela, R. K., Rengaswamy, R., Narasimhan, S., Sridhar, L. N., 2010. Recursive state estimation techniques for nonlinear differential algebraic systems. Chemical engineering science 65 (16), 4548–4556.

Pacharu, S. R., Gudi, R., Patwardhan, S., 2012. Advanced state estimation techniques for packed bed reactors. IFAC Proceedings Volumes 45 (15), 519–524.

Rangegowda, P. H., Patwardhan, S. C., Mukhopadhyay, S., 2020. Fault Tolerant Control of a Nuclear Steam Generator in the presence of Sensor Biases. IFAC-PapersOnLine 53 (1), 579–584.

Seth, G., Patwardhan, S. C., Bhushan, M., 2021. Estimation of Spatial Concentration Profiles in a Plug Flow Reactor using Reduced Dimensional Models. IFAC-PapersOnLine 53 (1), 39–44.

Valluru, J., Patwardhan, S. C., Biegler, L. T., 2018. Development of robust extended Kalman filter and moving window estimator for simultaneous state and parameter/disturbance estimation. Journal of Process Control 69, 158–178.